Self–Powered Magnetic Sensor Based on a Triboelectric Nanogenerator

6 **AUTHORS**, INCLUDING:

Ya Yang
Chinese Academy of Sciences
51 PUBLICATIONS **1,650** CITATIONS

Long Lin
Georgia Institute of Technology
58 PUBLICATIONS **2,080** CITATIONS

Yue Zhang
Fudan University
334 PUBLICATIONS **3,581** CITATIONS

Qingshen Jing
Peking University
37 PUBLICATIONS **1,443** CITATIONS

Self-Powered Magnetic Sensor Based on a Triboelectric Nanogenerator

Ya Yang,[†,⊥] Long Lin,[†,⊥] Yue Zhang,[‡] Qingshen Jing,[†] Te-Chien Hou,[†] and Zhong Lin Wang[†,§,*]

[†]School of Material Science and Engineering, Georgia Institute of Technology, Atlanta, Georgia 30332-0245, United States, [‡]State Key Laboratory for Advanced Metals and Materials, School of Materials Science and Engineering, University of Science and Technology Beijing, 100083 Beijing, China, and [§]Beijing Institute of Nanoenergy and Nanosystems, Chinese Academy of Sciences, China. [⊥]These authors contributed equally to this work.

ABSTRACT Magnetic sensors are usually based on the Hall effect or a magnetoresistive sensing mechanism. Here we demonstrate that a nanogenerator can serve as a sensor for detecting the variation of the time-dependent magnetic field. The output voltage of the sensor was found to exponentially increase with increasing magnetic field. The detection sensitivities for the change and the changing rate of magnetic field are about 0.0363 ± 0.0004 ln(mV)/G and 0.0497 ± 0.0006 ln(mV)/(G/s), respectively. The response time and reset time of the sensor are about 0.13 and 0.34 s, respectively. The fabricated sensor has a detection resolution of about 3 G and can work under low frequencies (<0.4 Hz).
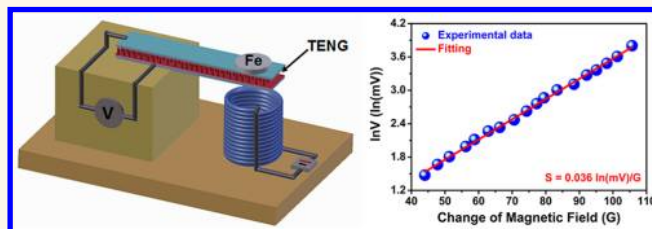
Nanogenerator (NG) is a technology that converts mechanical energy as produced by small-scale physical action into electricity.[1] NG has three typical approaches: piezoelectric,[2−4] triboelectric,[5,6] and pyroelectric nanogenerators.[7,8] If we take the output electric signal as a power source, it is the original objective of the NGs. Alternatively, the signal from NG can be used as a sensor to directly measure the magnitude and dynamic behavior of the mechanical triggering or temperature variation, which is a new type of active sensor for monitoring mechanical and thermal processes, such as vortex capture and ambient wind velocity detection,[9] low-frequency vibrations,[10] automobile velocity,[11] and temperature sensing.[12] There is an urgent need to develop self-powered nanotechnology that the NG is utilized as both the power source and the active sensor.[13−15]

Magnetic fields have many uses in ancient and modern society. The detection of magnetic field is important for environmental surveillance, mineral exploring, and safety monitoring. Currently, the reported magnetic sensors are usually based on the Hall effect sensing mechanism or magnetoresistive sensing mechanism.[16−18] In this study, we demonstrate the first application of the NG for sensing a time-dependent magnetic field without the use of an external power source. The output voltage of the sensor was found to exponentially increase with increasing the change of magnetic field, and the detection sensitivities for the change and the changing rate of magnetic field are about 0.0363 ± 0.0004 ln(mV)/G and 0.0497 ± 0.0006 ln(mV)/(G/s), respectively. The fabricated sensor has a response time of about 0.13 s and a reset time of about 0.34 s. The detection resolution and work frequencies of the sensor were also investigated.

RESULTS AND DISCUSSION

The triboelectric nanogenerator (TENG) used for this study was fabricated using a polydimethylsiloxane (PDMS) micro/nanowire array. The magnetic field B in a solenoid can be given by

$$B = \frac{\mu N I}{l} \quad (1)$$

where μ is the magnetic permeability, N is the number of turns, I is the current in the solenoid, and l is the height of loops of the solenoid.[19] In this study, the magnetic field to be sensed was produced by a solenoid, where the magnetic field increases with increasing both the number of loops and the current through the coils. The distribution of magnetic field in the coils was calculated by using the COMSOL software, as

© XXXX American Chemical Society
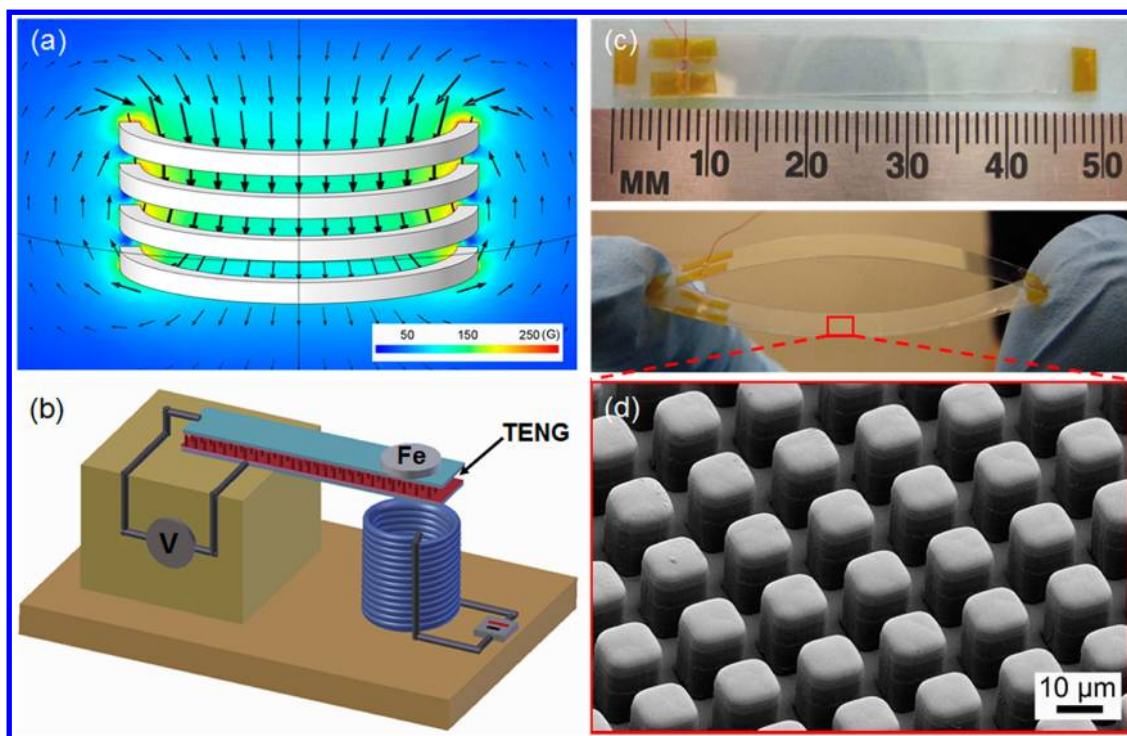
Figure 1. (a) Calculated magnetic field distribution in the coils. (b) Schematic diagram of the self-powered magnetic sensor and the corresponding measurement setup. (c) Photograph of the fabricated TENG device. (d) SEM image of the PDMS micropattern array.

shown in Figure 1a. The diameter of the used coils was about 0.05 m to produce the four rings with the diameter of 0.4 m. The distance between two adjacent coils is about 0.05 m, and the current density through the coils is about 1 A/mm^2. The obtained magnetic field is uniform in the center of the coils (about 100 G). Figure 1b shows a schematic of the fabricated self-powered magnetic sensor. One end of a flexible TENG was fixed. A metallic (Fe) disk was attached on the other end of the TENG as the sensitive unit of magnetic field, where a solenoid was put under the disk. When the current flows in the solenoid, the Fe disk is attracted by the electromagnetic force so that the TENG is bent downward, the deformation and deformation rate produced by which results in an electric output signal by TENG. The magnitude of the electric signal is an indication of the local magnetic field. This is the mechanism we will use to measure the magnetic field by using an electric signal.

The magnetic force between the Fe disk and the solenoid can be approximately expressed as

$$F_{mag} = kB\frac{dB}{dz} \qquad (2)$$

where k is the magnetic coefficient, z is the distance between the ferromagnetic object and the magnetic source, and B is the magnetic field.[20] The maximum deflection Z_m of the TENG can be given by

$$Z_m = \frac{F_{mag}L^3}{3YI} \qquad (3)$$

where Y is the elastic modulus of the TENG, I is the momentum of inertia, and L is the length of TENG from the fixed end to the free end.[21] By using eqs 2 and 3, we can see that the magnitude of bending of the TENG increases with increasing the magnetic field.

Figure 1c shows an optical image of the fabricated TENG, where the length and width of the TENG are about 50 and 5 mm, respectively. The structure of the TENG includes a PET film with the ITO top electrode and a PDMS micro/nanowire array with the ITO as the bottom electrode. The two parts were connected with a Kapton tape and can be easily bent, as shown in Figure 1c. The fabricated devices are transparent and flexible. Figure 1d shows the SEM image of the PDMS microwire array, indicating that the diameters of the PDMS wires are about 10 μm. The same principle and methodology can apply to a PDMS nanowire array. The detailed fabrication method of PDMS micro/nanowire array is given in the Experimental Section. The working mechanism of the TENG was reported previously.[5,6]

Figure 2a shows the change of magnetic field at the TENG as a self-powered sensor. Under forward connection, a sharp positive voltage/current pulse (22 mV/0.8 nA) was observed when the magnetic field was quickly increased from 0 to 88 G, as shown in Figure 2b. The output voltage peaks of the device nearly keep at the same values. After reversely connecting the sensor to the measurement system, the output signals were opposite (Figure 2c), indicating that the measured signals were generated by the fabricated sensor. Figure 2d shows the
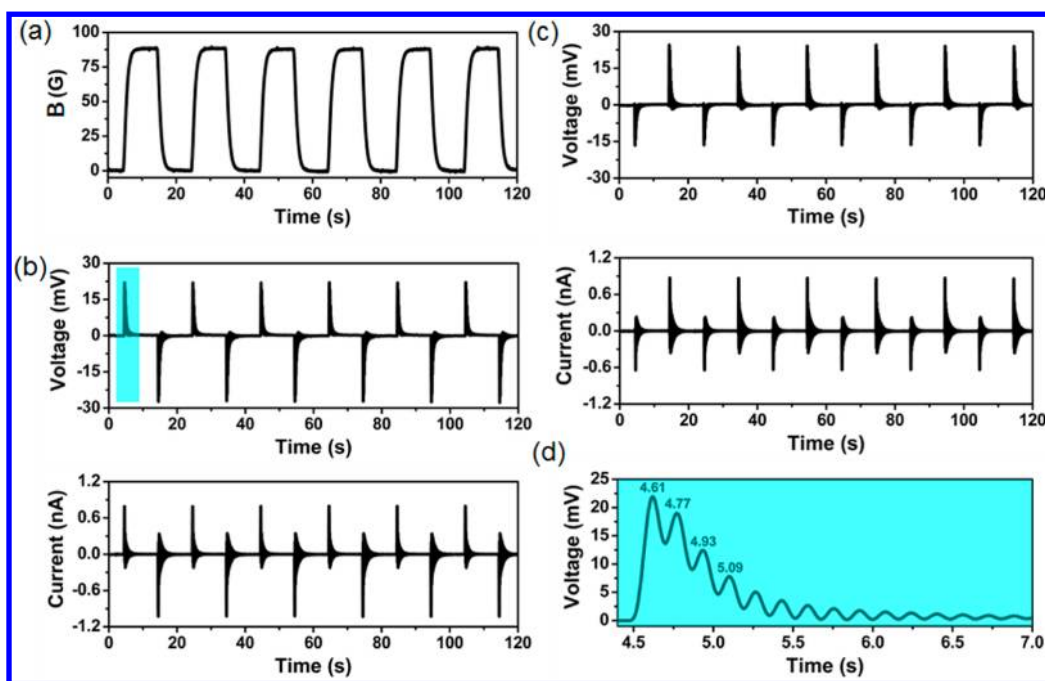
Figure 2. (a) Cyclic changes of the magnetic field *B* near the sensor. (b,c) Output voltage and current of the device at forward connection (b) and reversed connection (c) to the measurement system when it was subject to the change of the magnetic field in (a). (d) Enlarged first output voltage peak of the device in (b).
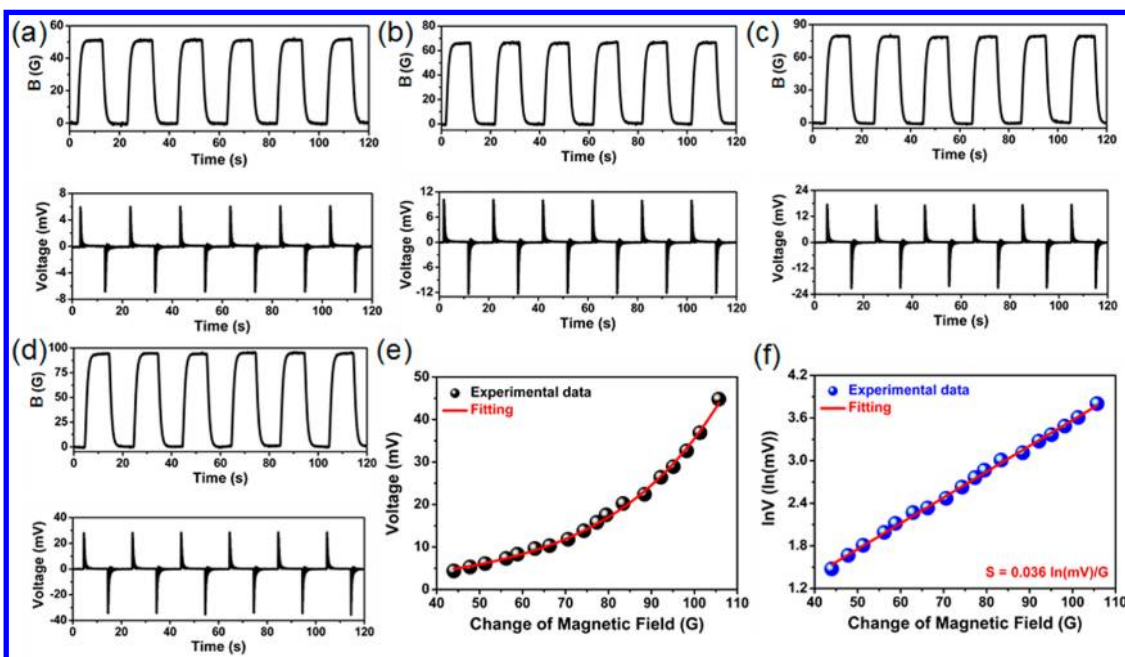

Figure 3. (a−d) Electrical output voltage of the sensor when it was subject to the cyclic change of the different magnetic fields. (e) Dependence of the output voltage of the sensor on the change of magnetic field *B*. (f) Plot showing the linear relationship between the ln*V* and *B*.

enlarged peak of the output voltage in Figure 2b. There are many small voltage oscillating peaks with a time interval of about 0.16 s, which are due to the free vibration of the TENG sensor as it is attracted by the magnetic forces between the Fe disk and the solenoid.

Figure 3a−d shows the output voltage of the sensor under the different changes of the magnetic field. It can be seen that the output voltage increases with

increasing the change of magnetic field. Figure 3e shows the measured voltage peaks as a function of the change in magnetic field, demonstrating an exponential relationship by fitting the data. Here, we investigated the mechanism of the self-powered TENG magnetic sensor. At original state, there is no electric potential difference between the two ITO electrodes. With the electromagnetic force introduced bending,

the contact status between PDMS and PET polymers was changed, resulting in the surface charge transfer due to triboelectric effect.[22] According to the different triboelectric coefficients,[23] electrons will be injected from PET into PDMS, resulting in net negative charges on the inner surface of PDMS and net positive charges on the inner surface of PET, respectively. The induced charges have a long-time retention due to the insulating property of the polymers.[24] The output voltage V_{oc} of the sensor can be given by

$$V_{oc} = \frac{\sigma d}{\varepsilon_0} \qquad (4)$$

where σ is the triboelectric charge density, d is the interlayer distance, and ε_0 is the vacuum permittivity.[6] The interlayer distance d corresponds to the deflection of the sensor (from 0 to Z_m). Both the triboelectric charge density σ and the interlayer distance d will increase with increasing the bending of the sensor. Although we cannot obtain the exact relationship between the output voltage V_{oc} and the magnetic field B, it can be clearly seen that the output voltage V_{oc} will increase with increasing magnetic field B by using eqs 1–4. For practical applications of the sensors, a linear relationship between the output and input signals is always preferred. We obtained the ln$V$–B curve in Figure 3f, showing a linear relationship. The corresponding sensitivity for the change of magnetic field was calculated to be about 0.0363 ± 0.0004 ln(mV)/ G by fitting the data points (the red curve in Figure 3f).

An important application of the fabricated magnetic sensor is that it can be used to detect the changing rate of the magnetic field. Figure 4a shows that the output voltage peak of the sensor is about 38 mV when the cyclic magnetic field changing rate is about 80 G/s. It is
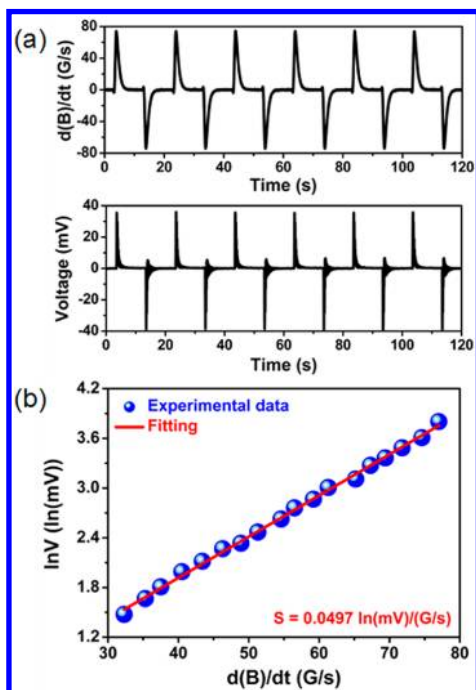

Figure 4. (a) Output voltage of the sensor under the cyclic change of magnetic field changing rate. (b) Dependence of the output voltage on the changing rate of the magnetic field.
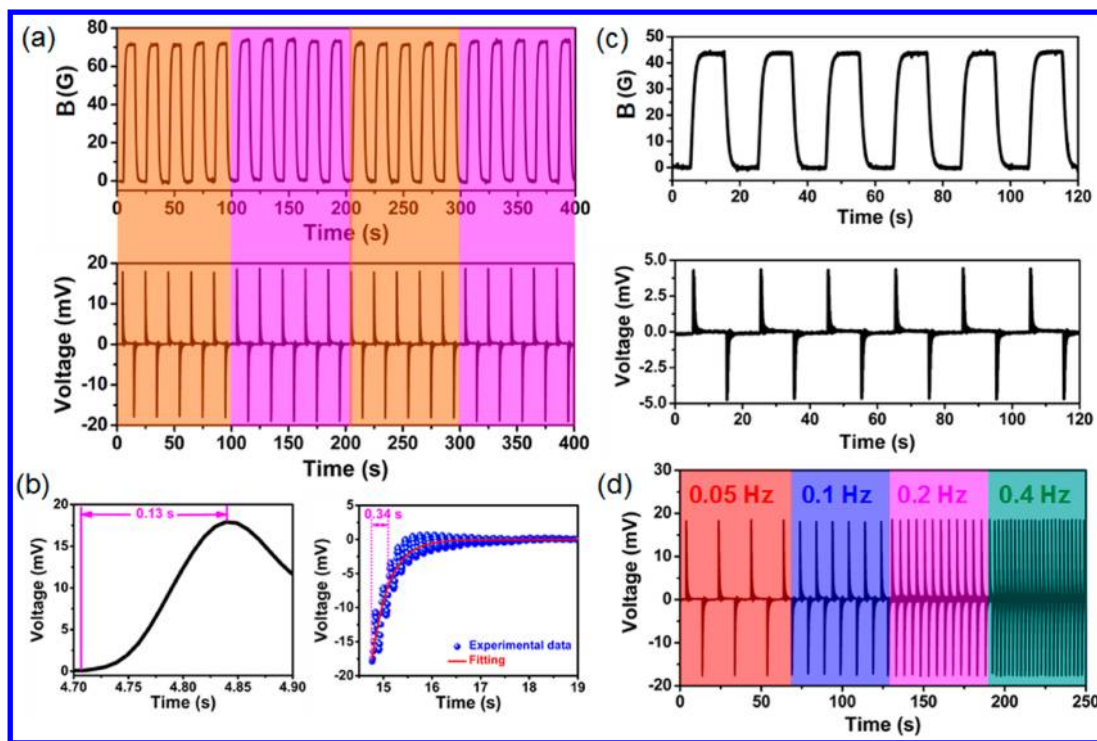

Figure 5. (a) Output voltage of the sensor under the two different changes of magnetic field B. (b) Response time and reset time of the sensor by enlarging the output signals in a. (c) Output voltage of the sensor under the minimum change of the magnetic field. (d) Output voltage of the sensor under the different working frequencies.

noticed that the voltage/current pulse signals generated when the magnetic field was changed from "on" to "off" are obviously larger than those generated when the magnetic field was changed from "off" to "on" in Figures 2 and 4, which is associated with the different deformation rates in the two processes. Although the peak of the changing rate of the magnetic field is consistent with the output voltage peak of the device, the width of the former is significantly larger than the latter, which is associated with the threshold changing rate of the magnetic field, below which there will be no observed output voltage signal. The $\ln V - dH/dt$ curve shows a linear relationship in Figure 4b, where the sensitivity of the changing rate of the magnetic field is about $0.0497 \pm 0.0006 \ln(mV)/(G/s)$.

In order to obtain the resolution of the magnetic field of the fabricated sensor, we measured the output voltages under the two adjacent changes of magnetic field, as shown in Figure 5a. The resolution of the magnetic field is about 3 G (74.35−71.35 G) for an output voltage difference of about 0.95 mV (18.91−17.96 mV), which is much larger than the equipment measurement noise signal of about 0.1 mV. Figure 5b shows the enlarged positive pulse signal in Figure 5a. The response time is about 0.13 s, where it was calculated from 0 to the maximum value of the output voltage pulse. When the magnetic field was off, an opposite pulse signal appeared and then returned to 0. The decay time of the fabricated sensor follows an exponential decay function with a time constant of 0.35 s by fitting the $V-T$ curve in Figure 5b. The calculated reset time of the sensor is about 0.34 s, where it is defined as the time needed to recover to 37%.[25] The response time and reset time of the fabricated magnetic sensor are much shorter than those of the conventional magnetic sensors.[16−18]

Figure 5c shows the output voltage of the self-powered sensor under a minimum change in magnetic field of 44 G, resulting in an observed output voltage peak of about 4.4 mV. It indicates that the sensor can be used to detect the change of magnetic field, which is larger than 44 G. When the change of magnetic field is below 44 G, the obtained signals are smaller than 5 mV.

However, they are noise signals since the reversed signals cannot be obtained when the device was under the reversed connection to the measurement system. These signals are related to the applied magnetic field. Figure 5d shows the output voltage of the sensor under different working frequencies from 0.05 to 0.4 Hz. It can be clearly seen that the output voltage of the sensor nearly remains at the same value under the different frequencies. The sensor can work at a range of low frequencies (<0.4 Hz). The higher frequencies will result in a decay of the output voltage of the sensor since the width of the output voltage pulse is about 2.5 s, as shown in Figure 2d. In this study, we used the PDMS−PET polymer TENG as a model to demonstrate that it can be used as a self-powered magnetic sensor. In the practical applications, there are two possible methods to improve the performance of the sensor further. One is to choose the polymer materials with a larger difference of triboelectric coefficients than that of PDMS−PET system, which can result in a larger output of the sensor under the same magnetic field change. The other method is to use the materials with lower elastic modulus, which can give a larger deflection of sensor under the same magnetic force conditions.

CONCLUSION

In summary, we have demonstrated the first application of a TENG as a self-powered sensor for detecting the change of magnetic field in a solenoid. The output voltage of the sensor was found to exponentially increase with increasing the change of magnetic field, where the detection sensitivities for the change and the changing rate of magnetic field are about $0.0363 \pm 0.0004 \ln(mV)/G$ and $0.0497 \pm 0.0006 \ln(mV)/(G/s)$, respectively. The response time and reset time of the sensor are about 0.13 and 0.34 s, respectively. The self-powered magnetic sensor has a detection resolution of about 3 G and can work at a range of low frequencies (<0.4 Hz). The self-powered magnetic sensors have potential applications for environmental surveillance, magnetic sensing, mineral exploring, and defense technology.

EXPERIMENTAL SECTION

Fabrication of TENGs. The TENG is made of two sheets of polymers (PET and PDMS) that have different triboelectric characteristics. To make the PDMS micro/nanowire array, a Si wafer mold was fabricated by a traditional photolithography method. To avoid the sticking of the PDMS, the surface of the mold was treated by using the trimethylchlorosilane. The liquid PDMS was dropped in the mold and was then put in a container, where the air was pumped out. The PDMS was then heated at the temperature of 85 °C in an oven and peeled off from the mold. The obtained PDMS micro/nanowire array was fixed on a clean ITO-coated PET substrate. Another ITO-coated PET substrate was put on the top of the PDMS micro/nanowire array to form a sandwich-structured device. The two ends of the structure were connected by using a Kapton tape, and the ITO films were used as the top and bottom electrodes.

Measurement of the Self-Powered Magnetic Sensor. One end of the sensor was fixed on a wooden body, and a metal (Fe) disk was attached on the other end, which was used as the sensitive unit of magnetic field. A solenoid was put under the Fe disk, where a DC voltage was applied on the solenoid. When the current flows in the solenoid, the magnetic force between the metal disk and the magnetic solenoid will bend the sensor, resulting in an observed output voltage/current. A magnetic sensor was used to record the magnetic field near the device during all experiments. The output performance of the fabricated sensor was measured by using a low-noise voltage preamplifier (Stanford Research System model SR560) and a low-noise current preamplifier (Stanford Research System Model SR570).

Conflict of Interest: The authors declare no competing financial interest.

REFERENCES AND NOTES

1. Wang, Z. L.; Song, J. H. Piezoelectric Nanogenerators Based on Zinc Oxide Nanowire Arrays. *Science* **2006**, *312*, 242–246.
2. Wang, X.; Song, J.; Liu, J.; Wang, Z. L. Direct-Current Nanogenerator Driven by Ultrasonic Waves. *Science* **2007**, *316*, 102–105.
3. Qin, Y.; Wang, X.; Wang, Z. L. Microfibre–Nanowire Hybrid Structure for Energy Scavenging. *Nature* **2008**, *451*, 809–813.
4. Zhu, G.; Yang, R.; Wang, S.; Wang, Z. L. Flexible High-Output Nanogenerator Based on Lateral ZnO Nanowire Array. *Nano Lett.* **2010**, *10*, 3151–3155.
5. Fan, F.-R.; Tian, Z.-Q.; Wang, Z. L. Flexible Triboelectric Generator. *Nano Energy* **2012**, *1*, 328–334.
6. Zhu, G.; Pan, C.; Guo, W.; Chen, C.-Y.; Zhou, Y.; Yu, R.; Wang, Z. L. Triboelectric-Generator-Driven Pulse Electrodeposition for Micropatterning. *Nano Lett.* **2012**, *12*, 4960–4965.
7. Yang, Y.; Guo, W.; Pradel, K. C.; Zhu, G.; Zhou, Y.; Zhang, Y.; Hu, Y.; Lin, L.; Wang, Z. L. Pyroelectric Nanogenerators for Harvesting Thermoelectric Energy. *Nano Lett.* **2012**, *12*, 2833–2838.
8. Yang, Y.; Jung, J. H.; Yun, B. K.; Zhang, F.; Pradel, K. C.; Guo, W.; Wang, Z. L. Flexible Pyroelectric Nanogenerators Using a Composite Structure of Lead-Free KNbO$_3$ Nanowires. *Adv. Mater.* **2012**, *24*, 5357–5362.
9. Zhang, R.; Lin, L.; Jing, Q.; Wu, W.; Zhang, Y.; Jiao, Z.; Yan, L.; Han, R. P. S.; Wang, Z. L. Nanogenerators as an Active Sensor for Vortex Capture and Ambient Wind-Velocity Detection. *Energy Environ. Sci.* **2012**, *5*, 8528–8533.
10. Yu, A.; Jiang, P.; Wang, Z. L. Nanogenerator as Self-Powered Vibration Sensor. *Nano Energy* **2012**, *1*, 418–423.
11. Lin, L.; Hu, Y.; Xu, C.; Zhang, Y.; Zhang, R.; Wen, X.; Wang, Z. L. Transparent Flexible Nanogenerator as Self-Powered Sensor for Transportation Monitoring. *Nano Energy* **2012**, DOI: 10.1016/j.nanoen.2012.07.019.
12. Yang, Y.; Zhou, Y.; Wu, J. M.; Wang, Z. L. Single Micro/Nanowire Pyroelectric Nanogenerators as Self-Powered Temperature Sensors. *ACS Nano* **2012**, *6*, 8456–8461.
13. Pan, C.; Li, Z.; Guo, W.; Zhu, J.; Wang, Z. L. Fiber-Based Hybrid Nanogenerators for/as Self-Powered Systems in Biological Liquid. *Angew. Chem., Int. Ed.* **2011**, *50*, 11192–11196.
14. Lee, M.; Bae, J.; Lee, J.; Lee, C.-S.; Hong, S.; Wang, Z. L. Self-Powered Environmental Sensor System Driven by Nanogenerators. *Energy Environ. Sci.* **2011**, *4*, 3359–3363.
15. Yang, Q.; Liu, Y.; Li, Z.; Yang, Z.; Wang, X.; Wang, Z. L. Self-Powered Ultrasensitive Nanowire Photodetector Driven by a Hybridized Microbial Fuel Cell. *Angew. Chem., Int. Ed.* **2012**, *51*, 6443–6446.
16. Johnson, M.; Bennett, B. R.; Yang, M. J.; Miller, M. M.; Shanabrook, B. V. Hybrid Hall Effect Device. *Appl. Phys. Lett.* **1997**, *71*, 974–976.
17. Guedes, A.; Patil, S. B.; Cardoso, S.; Chu, V.; Conde, J. P. Hybrid Magnetoresistive/Microelectromechanical Devices for Static Field Modulation and Sensor 1/*f* Noise Cancellation. *J. Appl. Phys.* **2008**, *103*, 07E924.
18. Pannetier, M.; Fermon, C.; Goff, G. L.; Simola, J.; Kerr, E. Femtotesla Magnetic Field Measurement with Magnetoresistive Sensors. *Science* **2004**, *304*, 1648–1650.
19. Scott, W. T. *The Physics of Electricity and Magnetism*; Wiley: New York, 1959.
20. Schenck, J. F. Safety of Strong, Static Magnetic Fields. *J. Magn. Reson. Imaging* **2000**, *12*, 2–19.
21. Song, J.; Zhou, J.; Wang, Z. L. Piezoelectric and Semiconducting Coupled Power Generating Process of a Single ZnO Belt/Wire. A Technology for Harvesting Electricity from the Environment. *Nano Lett.* **2006**, *6*, 1656–1662.
22. Nemeth, E.; Albrecht, V.; Schubert, G.; Simon, F. Polymer Triboelectric Charging: Dependence on Thermodynamic Surface Properties and Relative Humidity. *J. Electrostat.* **2003**, *58*, 3–16.
23. Cross, J. A. *Electrostatics: Principles, Problems and Applications*; Adam Hilger: Bristol, UK, 1987.
24. Saurenbach, F.; Wollmann, D.; Terris, B. D.; Diaz, A. F. Force Microscopy of Ion-Containing Polymer Surfaces: Morphology and Charge Structure. *Langmuir* **1992**, *8*, 1199–1203.
25. Yang, Y.; Pradel, K. C.; Jing, Q.; Wu, J. M.; Zhang, F.; Zhou, Y.; Zhang, Y.; Wang, Z. L. Thermoelectric Nanogenerators Based on Single Sb-Doped ZnO Micro/Nanobelts. *ACS Nano* **2012**, *6*, 6984–6989.